Fabrication of nitrogen-rich three-dimensional porous carbon composites with nanosheets and hollow spheres for efficient supercapacitor

Jinghua Liu[a], Xiaohui Ren[a], Xu Kang[b], Xiong He[a], Peicheng Wei[a], Yan Wen[b] and Xin Li[a,*]

[a]*MIIT Key Laboratory of Critical Materials Technology for New Energy Conversion and Storage, School of Chemistry and Chemical Engineering, State Key Lab of Urban Water Resource and Environment, Harbin Institute of Technology, Harbin 150090, China.*

[b]*School of Environment, Harbin Institute of Technology, Harbin 150090, China*

*Corresponding author: Tel.: +86-0451-86282153.

E-mail address: lixin@hit.edu.cn (X. Li)

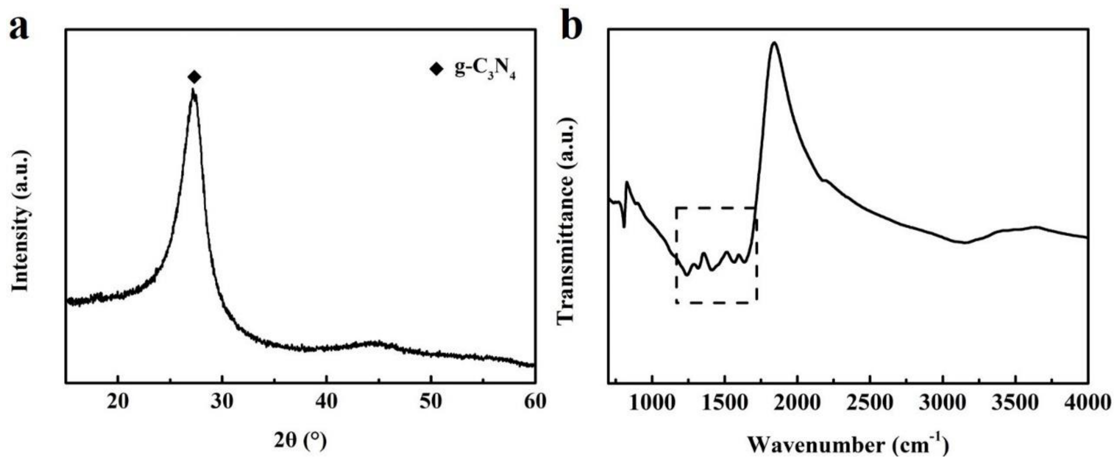

Fig. S1 (a) XRD pattern, (b) FT-IR spectrum of NCN/NHCS-550.

As shown in Fig. S1a, diffraction peak at 27.4° can be indexed as the respective (002) plane of g-C_3N_4, indicating the presence of g-C_3N_4 in the intermediate calcined at 550 °C[1]. In addition, the FT-IR spectrum further confirms the existence of g-C_3N_4 in the intermediate. As shown in Fig. S1b, the peak at 810 cm^{-1} is related to the triazine breathing vibration. All of the peaks in the 1200-1700 cm^{-1} region are derived from typical C-N heterocyclic stretches of the triazine (C_6N_7) ring[2]. Absorbance ranging from 3000 to 3400 cm^{-1} is associated with the N-H and O-H groups, suggesting the formation of g-C_3N_4 at 550 °C.

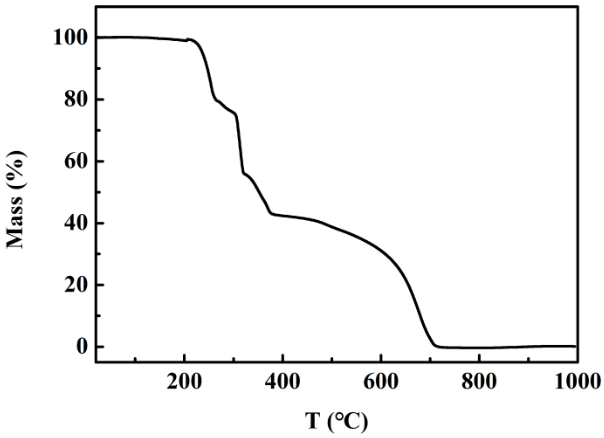

Fig. S2 TGA curve of DCDA in N_2 from room temperature to 1000 ℃.

Fig. S2 shows the TGA curve of DCDA in N_2 atmosphere from room temperature to 1000 ℃. It can be seen that DCDA suffers severe mass loss before 720 °C. With increasing the calcination temperature, DCDA gradually transformed to melamine, tris-s-triazine, and g-C_3N_4 in the range of 210-640 °C. Then, g-C_3N_4 undergoes thorough decomposition until 720 °C[3].

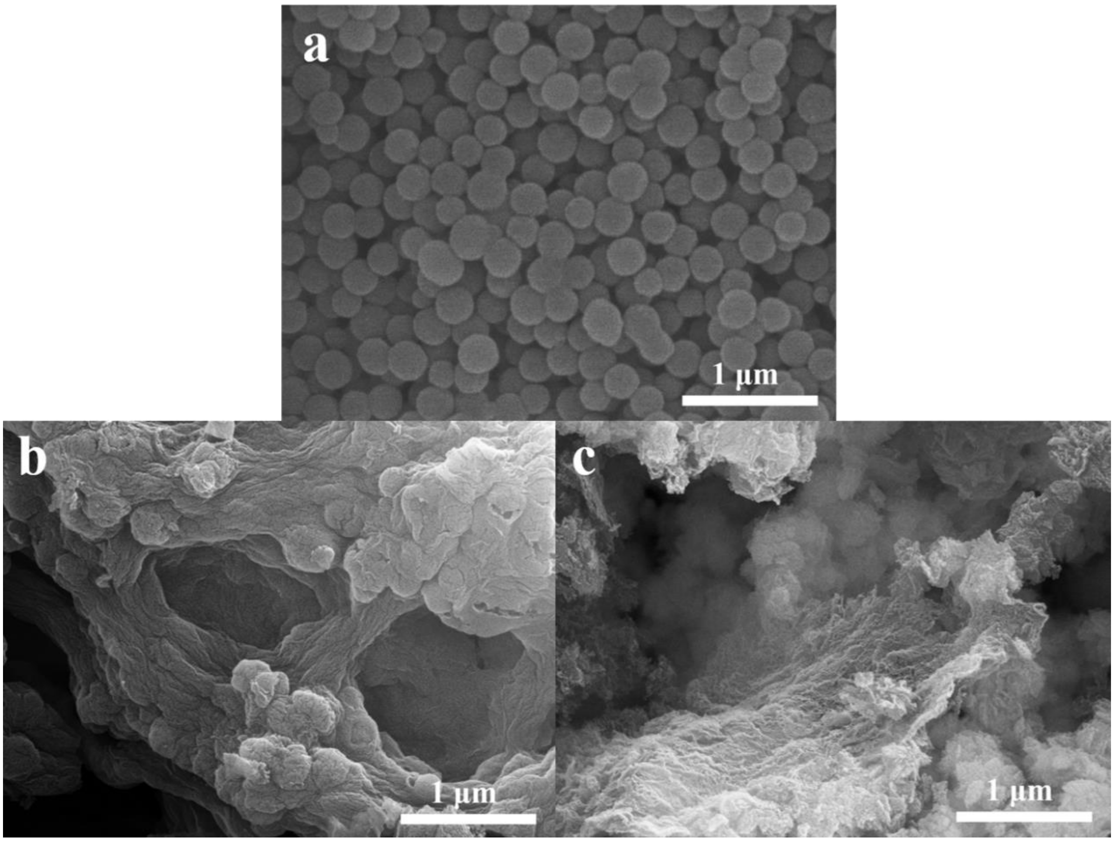

Fig. S3 SEM image of PDA@SiO_2 (a), NCN/NHCS-700 (b), and NCN/NHCS-900 (c).

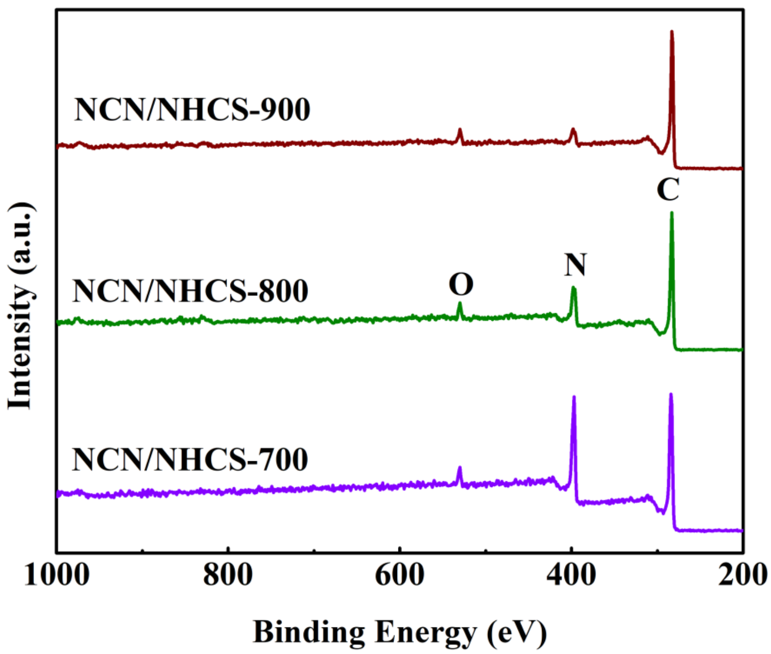

Fig. S4 XPS spectra of NCN/NHCS-Ts.

Table S1 The content (wt%) of C, N, and O elements in NCN/NHCS-Ts.

Sample	C (wt%)	N (wt%)	O (wt%)
NCN/NHCS-700	63.3	32.1	4.6
NCN/NHCS-800	72.1	23.2	4.7
NCN/NHCS-900	84.6	9.6	5.8

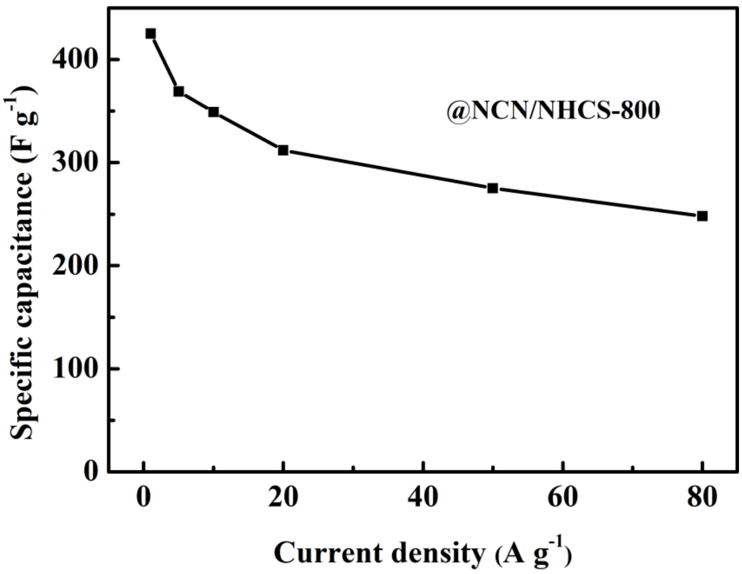

Fig. S5 Relationship between the specific capacitance and the current densities from 1-80 A g^{-1} for NCN/NHCS-800.

Table S2 Summary of the recently reported N-doped carbon materials and their electrochemical performances in three-electrode configurations.

Materials	V	Electrolytes	Capacitance
N-doped mesoporous carbon sheets [4]	-1 - 0	6 M KOH	232 F g^{-1} at 0.5 A g^{-1}
Porous N-doped carbon [5]	-1 - 0	6 M KOH	350.8 F g^{-1} at 1 A g^{-1}
N-rich graphene-like carbon sheets [6]	-1 - 0	6 M KOH	261 F g^{-1} at 1 A g^{-1}
Super-hierarchical porous carbons [7]	-1 - 0	6 M KOH	420 F g^{-1} at 0.5 A g^{-1}
N-doped hollow carbon nanospheres [8]	0 - 0.8	1 M H_2SO_4	240 F g^{-1} at 1 A g^{-1}
N-doped mesoporous carbon spheres [9]	-1 - 0	6 M KOH	288 F g^{-1} at 0.1 A g^{-1}
N-doped carbon polyhedrons/sheets [10]	-0.2 - 0.8	1 M H_2SO_4	495.0 F g^{-1} at 0.1 A g^{-1}
N-doped hollow carbon spheres [11]	-1 - 0	6 M KOH	436.5 F g^{-1} at 0.5 A g^{-1}
this work	-1.0 - 0	6 M KOH	425 F g^{-1} at 1 A g^{-1}

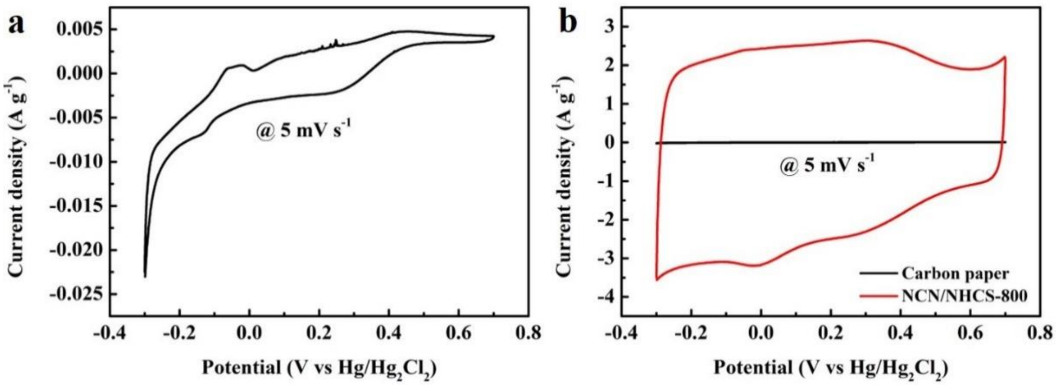

Fig. S6 (a) CV curve of carbon paper current collector at a scan rate of 5 mV s^{-1}, (b) CV curves of carbon paper current collector compared with NCN/NHCS-800 at a scan rate of 5 mV s^{-1}.

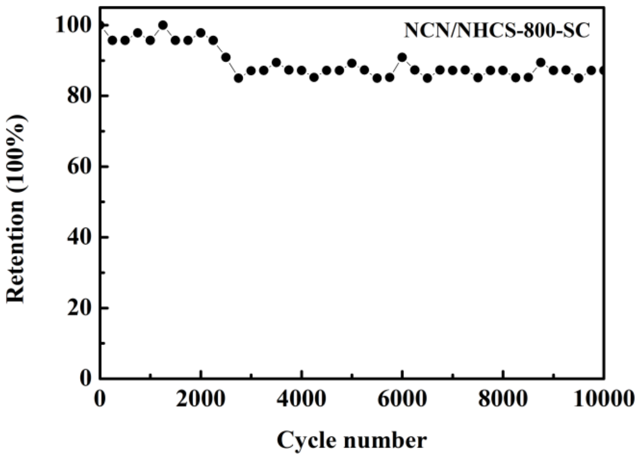

Fig. S7 Cycling performance of NCN/NHCS-800-SC at the current density of 10 A g^{-1} in two-electrode system.

References

[1] X.H. Li, S. Kurasch, U. Kaiser, M. Antonietti, Synthesis of Monolayer-Patched Graphene from Glucose, Angew. Chem.-Int. Edit. 51(38) (2012) 9689-9692.

[2] W. Xing, W. Tu, Z. Han, Y. Hu, Q. Meng, G. Chen, Template-induced high-crystalline g-C_3N_4 nanosheets for enhanced photocatalytic H2 evolution, ACS Energy Letters 3(3) (2018) 514-519.

[3] A. Thomas, A. Fischer, F. Goettmann, M. Antonietti, J.O. Muller, R. Schlogl, J.M. Carlsson, Graphitic carbon nitride materials: variation of structure and morphology and their use as metal-free catalysts, Journal of Materials Chemistry 18(41) (2008) 4893-4908.

[4] Y.N. Hou, Z.B. Zhao, Z.F. Yu, S. Zhang, S.F. Li, J. Yang, H. Zhang, C. Liu, Z.Y. Wang, J.S. Qiu, Microporous MOFs Engaged in the Formation of Nitrogen-Doped Mesoporous Carbon Nanosheets for High-Rate Supercapacitors, Chem.-Eur. J. 24(11) (2018) 2681-2686.

[5] K.X. Zou, Y.F. Deng, J.P. Chen, Y.Q. Qian, Y.W. Yang, Y.W. Li, G.H. Chen, Hierarchically porous nitrogen-doped carbon derived from the activation of agriculture waste by potassium hydroxide and urea for high-performance supercapacitors, Journal of Power Sources 378 (2018) 579-588.

[6] W. Yang, L.Q. Hou, X.W. Xu, Z.H. Li, X.L. Ma, F. Yang, Y.F. Li, Carbon nitride template-directed fabrication of nitrogen-rich porous graphene-like carbon for high performance supercapacitors, Carbon 130 (2018) 325-332.

[7] L. Peng, Y.R. Liang, H.W. Dong, H. Hu, X. Zhao, Y.J. Cai, Y. Xiao, Y.L. Liu, M.T. Zheng, Super-hierarchical porous carbons derived from mixed biomass wastes by a stepwise removal strategy for high-performance supercapacitors, Journal of Power Sources 377 (2018) 151-160.

[8] C. Liu, J. Wang, J. Li, M. Zeng, R. Luo, J. Shen, X. Sun, W. Han, L. Wang, Synthesis of N-doped hollow-structured mesoporous carbon nanospheres for high-performance supercapacitors, ACS applied materials & interfaces 8(11) (2016) 7194-7204.

[9] J.G. Wang, H.Z. Liu, H.H. Sun, W. Hua, H.W. Wang, X.R. Liu, B.Q. Wei, One-pot synthesis of nitrogen-doped ordered mesoporous carbon spheres for high-rate and long-cycle life supercapacitors, Carbon 127 (2018) 85-92.

[10] L.R. Kong, Q.R. Chen, X.P. Shen, Z.Y. Xu, C. Xu, Z.Y. Ji, J. Zhu, MOF derived nitrogen-doped carbon polyhedrons decorated on graphitic carbon nitride sheets with enhanced electrochemical capacitive energy storage performance, Electrochimica Acta 265 (2018) 651-661.

[11] J. Du, L. Liu, Y. Yu, Z. Hu, Y. Zhang, B. Liu, A. Chen, Tuning Confined Nanospace for Preparation of N-doped Hollow Carbon Spheres for High Performance Supercapacitors, ChemSusChem 12(1) (2019) 303-309.